The 2010 IEEE/RSJ International Conference on
Intelligent Robots and Systems
October 18-22, 2010, Taipei, Taiwan

Actuation Model for Control of a Long Range Lorentz Force Magnetic Levitation Device

Peter Berkelman and Michael Dzadovsky

Abstract— **This paper describes control system development for a large motion range Lorentz force magnetic levitation device designed as a haptic interface device to be grasped by the hand. Due to the 50 mm translation and 60 degree rotation motion ranges of the desktop-sized device, the transformation between the vector of coil currents and the actuation forces and torques generated on the levitated body varies significantly throughout its motion range. To improve the dynamic performance of the device, the current to force and torque transformation can be recalculated at each control update as the levitated body moves about its workspace, rather than using a constant transformation calculated from the unrotated and centered position of the levitated body. The design of the device is presented and the new methods used to calculate coil current to force and torque transformations for levitation are described. Long-range trajectory following feedback control motion results are shown.**

I. INTRODUCTION

The primary application of Lorentz levitation devices has been for haptic interaction, in which a levitated handle grasped by a user reproduces the dynamic physical behavior of a rigid tool interacting with a remote or virtual environment. The advantages of magnetic levitation for haptic interaction are its full six degree-of-freedom rigid body motion capabilities with a single moving part, high control bandwidths and impedance range, and frictionless backdriveable motion. Increasing the maximum translation and rotation ranges of Lorentz levitation devices to 50 mm and 60 degrees more closely approximates the motion range of grasped objects manipulated by the fingers and wrist, which enables the interactive simulation of tool manipulation tasks such as mechanical assembly and surgical training without the need for scaling or indexing.

Lorentz force magnetic levitation uses the forces generated from electric currents passing through magnetic fields to levitate a rigid body. Optical position sensing is used for feedback control. With a thin coil on a flat or spherically curved surface in a magnetic field, the Lorentz force generated between the coil and magnet assembly is:

$$\mathbf{f} = \int \mathbf{B} \times \mathbf{I}\, dl, \tag{1}$$

acting through the centroid of the coil, where $\mathbf{B}$ is the magnetic flux density, $\mathbf{I}$ is the electrical current, and l is the total length of the wire passing through the field, integrated along its length in the field.

This work was supported by the National Science Foundation awards #CNS05-51515 and#IIS08-46172.

Peter Berkelman and Michael Dzadovsky are with the Department of Mechanical Engineering, University of Hawaii-Manoa, Honolulu, HI 96822, USA, peterb@hawaii.edu, dzadovsk@hawaii.edu

TABLE I
MOTION RANGES OF HAPTIC MAGNETIC LEVITATION DEVICES

Device	Translation	Rotation
IBM Magic Wrist	10 mm	6°
UBC Teleoperation Master	10 mm	6°
UBC Powermouse	2.5 mm	10°
CMU/Butterfly Haptics	25-30 mm	15-20°
Ohio State University	2 mm	2°
University of Hawaii	50 mm	60°

To levitate a single rigid body with 6 degrees of freedom (DOF) in translation and rotation, 6 coils must be embedded in the rigid body, arranged in a configuration so that arbitrary vector forces and torques can be produced by the actuator coils acting in combination. The advantage of Lorentz forces rather than electromagnetic attraction or repulsion for levitation is that the actuation forces generated are linearly dependent only on the coil current, the magnetic field flux density, and the length of the wire passing through the magnetic field.

The novel design of the device, as described in Section III, allows a much greater motion range than previous Lorentz levitation devices, and the small angle approximations and constant matrix transformation actuation force and torque models previously used are no longer sufficient for accurate motion throughout the range of the device. The improvements in the accuracy of the force and torque actuation model are described in Section IV, followed by results and discussion, and conclusions and further work.

II. BACKGROUND

Lorentz force magnetic levitation devices were invented by Hollis and Salcudean [1], leading to the development of the *IBM Magic Wrist* [2], a robotic wrist for compliant assembly. Salcudean developed the *Teleoperation Master* [3] for force-feedback teleoperation, and the *Powermouse* [4] for force-feedback human-computer interaction. Berkelman and Hollis [5] developed a larger range-of-motion Lorentz levitation device which was developed further into the *Maglev 200*[1] magnetic levitation haptic interface. Zhang and Menq [6] have developed a Lorentz levitation device with a different magnet and coil configuration, for nanometer-scale precision motion rather than haptic interaction. The motion ranges of these devices are given in Table 1. Preliminary design studies of the University of Hawaii device described here are given in [7] and initial levitation results in [8].

[1]Butterfly Haptics LLC

All of these Lorentz levitation devices have been controlled using a constant current to force and torque transformation matrix calculated from the center, unrotated position of the levitated body, which has been sufficient for stable levitation control over their translation and rotation ranges. Variations in force generation along the vertical direction of motion were experimentally measured for calibration of the Butterfly Haptics device by Varadharajan [9], and potential improvements in spatial rigid-body orientation stiffness and damping control are described by Fasse [10].

III. DEVICE DESIGN

In this device, the six coils on the levitated body conform to a thin spherical shell with a user interaction handle fixed at its center, and stationary magnets are fixed inside and outside of the shell to generate magnetic fields through the coils normal to the shell surface when the levitated body is in the center of its motion range, in a configuration similar to the CMU/Butterfly Haptics devices developed previously. The design of the device is shown in Fig. 1. This new device uses an original coil shape in which the windings follow straight paths across the centers of the coils and return along the circumference of the circular coils. This allows the coils to be arranged in two layers with the wire paths orthogonal to one another across the centers of the coils, as shown in Fig. 2. The coils were wound by hand, using curved guides, tacks, and epoxy to attain the desired shape with the wires across the center packed together as closely as possible.

In this arrangement, the active areas of the coils can be maximized without increasing the radius of the spherical shell, and each pair of layered coils requires only two magnets to generate their shared magnetic field. Curved iron pole pieces pass above and around the coils to guide and concentrate the flux between each magnet pair, while allowing the user to grasp and manipulate the handle at the center of the levitated shell.

The radius of the coil sphere is 125 mm, the coil centers are at an inclination of -35 degrees from the horizontal plane through the sphere's center at 120 degree intervals about the circumference, and each coil subtends a 90 degree angle on the sphere. The effective angle of each coil is reduced to approximately 70 degrees due to the width of the magnets and the return paths of the wires around the edges of the coils. As a result the levitated body can be rotated at least 60 degrees in any direction, or ± 30 degrees from zero rotation, without moving any coil out of the region of its magnetic field.

The gaps between the magnet faces are at least 53 mm and the thickness of the levitated shell is approximately 3 mm, resulting in a 50 mm translation range in all directions. The levitated mass is approximately 1100 g. Compared to the CMU/Butterfly Haptics devices which levitate a spherical shell of a similar size, the increased active areas of the coils made possible by their novel shape and arrangement in two layers result in a threefold increase in the rotation range, and the magnet assembly design with a single air gap and two coils in each flux path results in approximately double the translation range, or 8 times the motion volume and 27 times the reachable orientation set.

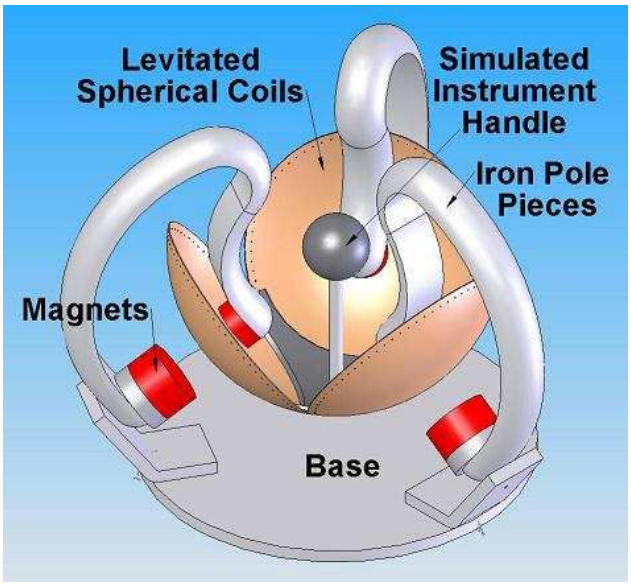

Fig. 1. Magnetic Leviation Device Design

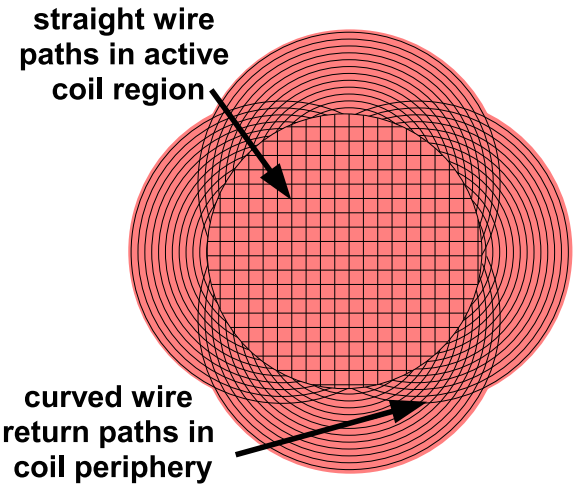

Fig. 2. Magnetic Leviation Device Design

A. Actuation

3D finite element analysis[2] was performed to determine magnet shapes and dimensions to concentrate and maximize magnetic flux for effective levitation. The component of the magnetic flux density normal to the magnet faces in between the magnets is shown in Fig. 3. The calculated minimum flux density between magnets is approximately 0.25 T, which has been shown [5] to be sufficient for Lorentz levitation. Gaussmeter measurements on the fabricated magnet assemblies confirm the accuracy of the analysis.

Actuation forces are generated from the coil areas passing through a magnetic field and depend on the direction of the

[2]Ansys Emag

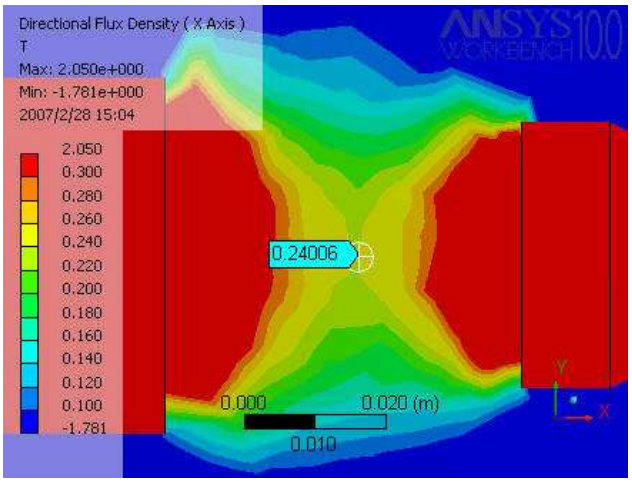

Fig. 3. Magnet Assembly Finite Element Analysis

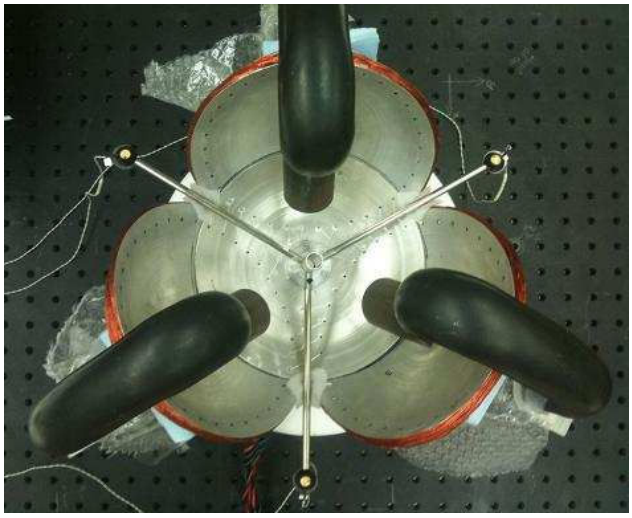

Fig. 4. Position Markers for Levitation Control

coil wires, the coil current, and the magnetic field direction, according to (1). The force generated by each coil can be modelled as a single force vector, and the two coils in each pair generate forces in perpendicular directions. The magnitude of the force generated by each coil is approximately 3.0 Newtons/Ampere. Each coil force $\mathbf{f}_i$ also produces a torque $\mathbf{r}_i \times \mathbf{f}_i$ about the center of the levitated body according to its location $\mathbf{r}_i$ on the spherical shell. Combining the force and torque generated by each of the six coils, the coil current to levitation force and torque vector transformation for the device can be given as:

$$\begin{bmatrix} f_x \\ f_y \\ f_z \\ \tau_x \\ \tau_y \\ \tau_z \end{bmatrix} = \begin{bmatrix} \mathbf{f_1} & \mathbf{f_2} & \cdots \\ \mathbf{r_1} \times \mathbf{f_1} & \mathbf{r_2} \times \mathbf{f_2} & \cdots \end{bmatrix} \begin{bmatrix} i_1 \\ i_2 \\ i_3 \\ i_4 \\ i_5 \\ i_6 \end{bmatrix}. \quad (2)$$

to relate currents in Amperes to forces in Newtons and torques in Newton-meters. If the transformation matrix between the six coil currents and the 3D force and torque vectors generated on the levitated body is invertible, and the required currents for levitation can be generated without overheating the coils, then the system can be levitated. Coil currents are generated by current amplifiers[3] controlled by a PC control system with a 1000 Hz update rate.

B. Position Sensing

Rigid-body position and orientation feedback is provided in real time at 1000 Hz by a 0.01 mm resolution optical position tracking sensor[4] mounted to a rigid frame above the levitated body. This position sensor detects the positions of three strobing infrared LED markers fixed to the rigid body and calculates its spatial position and orientation. The rigid body orientation may be calculated as either quaternion or rotation matrix forms.

[3]Copley Controls Corp. 4212Z
[4]Northern Digital Inc. Optotrak Certus Motion Capture System

In order for all three LED markers on the levitated bowl to be visible to the position sensor without being occluded by the iron pole pieces throughout the full motion range of the bowl, the markers are attached to lightweight, stiff hollow rods which extend 160 mm radially from the central axis of the bowl, as shown in Fig. 4. The large separation of the LED markers produces more accurate orientation sensing, however uncontrollable vibrations may be generated in the hollow rods during levitation. The vibrations have been minimized by introducing a thin layer of foam wrap between the edges of the coils and the position marker rods for to dampen vibrations in the levitated body and marker rods.

IV. CALCULATING CURRENT TO FORCE/TORQUE TRANSFORMS

When the levitated shell is in the centered position with zero rotation, the center axis of each magnetic field intersects the center of each coil and is normal to the spherical shell surface. The current to force and torque transformation (2) from this position and orientation can be used for stable levitation throughout the motion range, but the accuracy and performance of the controlled motion degrades with increased displacements and rotation angles. The variations in the actual current to force and torque transformations depend both on changes in the locations of the coil areas intersecting the magnetic fields as the levitated shell is translated, and changes in the directions of the coil currents as the shell is rotated.

When the levitated body moves from the center position, the magnetic field axes no longer intersect the center of each coil and they are no longer perpendicular to the shell surface, as shown in Fig. 5. To find the points $\mathbf{P_i}$ on the spherical shell intersected by the central axes of the three magnetic fields, we apply the line-sphere intersection formula [11]:

The surface of the spherical shell is described by

$$|\mathbf{P_i}|^2 = \rho^2, \quad (3)$$

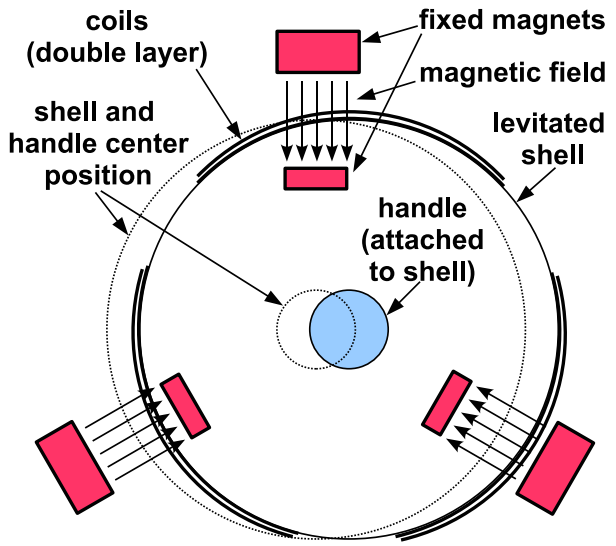

Fig. 5. Force Generation Schematic

where ρ is the 0.125 m sphere radius, and the fixed magnetic field axes relative to the center of the moving sphere can be described parametrically as

$$\mathbf{P_i} = -\mathbf{P_o} + d_i \hat{\mathbf{B}}_\mathbf{i}, \tag{4}$$

where $\mathbf{P_o}$ is the sensed displacement of the levitated body, d_i are scalar parameters, and $\hat{\mathbf{B}}_\mathbf{i}$ are unit vectors indicating the directions of the magnetic field axes. The intersection points are found by substituting the expressions for $\mathbf{P_i}$ (4) into the sphere surface equation (3) and solving d_i for each magnetic field axis $\hat{\mathbf{B}}_\mathbf{i}$:

$$|\mathbf{P_o}|^2 + {d_i}^2 {\hat{\mathbf{B}}_\mathbf{i}}^2 - 2d_i(\hat{\mathbf{B}}_\mathbf{i} \cdot \mathbf{P_o}) - 0.125^2 = 0 \tag{5}$$

by selecting the positive solutions to the quadratic formula

$$d_i = \hat{\mathbf{B}}_\mathbf{i} \cdot \mathbf{P_o} + \sqrt{(\hat{\mathbf{B}}_\mathbf{i} \cdot \mathbf{P_o})^2 - |\mathbf{P_o}|^2 + 0.125^2} \tag{6}$$

where the directions of the magnetic field axes are

$$\hat{\mathbf{B}}_{\mathbf{1,2}} = \begin{bmatrix} cos(35) \\ 0 \\ -sin(35) \end{bmatrix}, \hat{\mathbf{B}}_{\mathbf{3,4}} = \begin{bmatrix} cos(120)cos(35) \\ sin(120)cos(35) \\ -sin(35) \end{bmatrix}, \hat{\mathbf{B}}_{\mathbf{5,6}} = \begin{bmatrix} cos(240)cos(35) \\ sin(240)cos(35) \\ -sin(35) \end{bmatrix}, \tag{7}$$

which are constant as the magnet assemblies are fixed to the base. The locations of the magnetic field axis intersection points $\mathbf{x_i}$ on the coils relative to the sphere center are then given by substituting d_i into (4).

The directions of the two coil currents at the points of intersection of the sphere with the magnetic field axes are both tangent to the sphere surface. If the levitated body has zero rotation, then one direction at each intersection point $(\hat{I}_{01}, \hat{I}_{03}, \hat{I}_{05})$ is in the horizontal plane and the other direction in each coil pair $(\hat{I}_{02}, \hat{I}_{04}, \hat{I}_{06})$ is orthogonal to the first one:

$$\hat{\mathbf{I}}_{\mathbf{01}} = \begin{bmatrix} -P_{1y}/\sqrt{P_{1x}^2 + P_{1y}^2} \\ P_{1x}/\sqrt{P_{1x}^2 + P_{1y}^2} \\ 0 \end{bmatrix}, \hat{\mathbf{I}}_{\mathbf{02}} = \hat{\mathbf{P}}_\mathbf{1} \times \hat{\mathbf{I}}_{\mathbf{01}},$$
$$\hat{\mathbf{I}}_{\mathbf{03}} = \begin{bmatrix} -P_{3y}/\sqrt{P_{3x}^2 + P_{3y}^2} \\ P_{3x}/\sqrt{P_{3x}^2 + P_{3y}^2} \\ 0 \end{bmatrix}, \hat{\mathbf{I}}_{\mathbf{04}} = \hat{\mathbf{P}}_\mathbf{3} \times \hat{\mathbf{I}}_{\mathbf{03}},$$
$$\hat{\mathbf{I}}_{\mathbf{05}} = \begin{bmatrix} -P_{5y}/\sqrt{P_{5x}^2 + P_{5y}^2} \\ P_{5x}/\sqrt{P_{5x}^2 + P_{5y}^2} \\ 0 \end{bmatrix}, \hat{\mathbf{I}}_{\mathbf{06}} = \hat{\mathbf{P}}_\mathbf{5} \times \hat{\mathbf{I}}_{\mathbf{05}}. \tag{8}$$

The orientation of the levitated sphere affects the directions of the coil currents $\hat{\mathbf{I}}_\mathbf{i}$, although it does not affect the locations where the magnetic field axes intersect the surface of the sphere. The current direction unit vectors rotate around axes normal to the shell surface at the intersection points $\hat{\mathbf{P}}_\mathbf{i}$ by angles θ_i which depend on the overall rotation angle of the levitated body θ and the difference between the levitated body's rotation axis and the normal axis:

$$\theta_i = (\hat{\mathbf{k}} \cdot \hat{\mathbf{P}}_\mathbf{i})\theta, \tag{9}$$

where $\hat{\mathbf{k}}$ is the rotation axis and θ the rotation angle obtained from the quaternion orientation output of the position sensor. To rotate each current direction vector $\hat{\mathbf{I}}_\mathbf{i}$ about its corresponding surface normal $\hat{\mathbf{P}}_\mathbf{i}$ by angle θ_i, the Rodrigues rotation formula is applied:

$$\hat{\mathbf{I}}_\mathbf{i} = \hat{\mathbf{I}}_{\mathbf{i0}} cos\theta_i + sin\theta_i(\hat{\mathbf{k}} \times \hat{\mathbf{I}}_{\mathbf{i0}}) + (1 - cos\theta_i)(\hat{\mathbf{k}} \cdot \hat{\mathbf{I}}_{\mathbf{i0}})\hat{\mathbf{k}}. \tag{10}$$

Substituting the forces and torques generated into (2) produces the transformation matrix

$$\mathbf{A} = \begin{bmatrix} 3.0(\hat{\mathbf{B}}_\mathbf{1} \times \hat{\mathbf{I}}_\mathbf{1}) & 3.0(\hat{\mathbf{B}}_\mathbf{2} \times \hat{\mathbf{I}}_\mathbf{2}) & \cdots \\ 3.0(\mathbf{P_1} \times (\hat{\mathbf{B}}_\mathbf{1} \times \hat{\mathbf{I}}_\mathbf{1})) & 3.0(\mathbf{P_2} \times (\hat{\mathbf{B}}_\mathbf{2} \times \hat{\mathbf{I}}_\mathbf{2})) & \cdots \end{bmatrix} \tag{11}$$

between the coil current vector and the force and torque vector.

The force and torque vectors which compose the transformation matrix $\mathbf{A}$ generally rotate with the levitated body, and their magnitudes and directions also vary depending on the levitated body position as the orientations of the coil surfaces and magnetic fields change relative to each other. With a maximum rotation of 30 degrees in any direction, the components of each vector relative to its magnitude can vary by a factor of approximately $cos(30)$ or 0.5 over the motion range of the levitated body. The transformation matrix is invertible over the full motion range however, as the directions of the forces and torques from each coils always cover the full 3D vector space.

V. LEVITATION CONTROL

For position and orientation control of the levitated body, proportional and derivative error feedback (PD) control is

TABLE II
CONTROL GAINS

Gain	K_p	K_d
Translation	3.0 N/mm	0.075 N/(mm/sec)
Rotation	5.0 N-m/radian	0.40 N-m/(rad/sec)

applied to each DOF. A feedforward force equal to the weight of the levitated body is applied in the vertical direction to counteract gravity, and feedforward torques are applied according to the orientation of of the levitated body to counteract gravitational torques at the center point because the center of mass of the levitated bowl is below its center of curvature. Coil currents are generated from the calculated transformation matrix and the forces and torques from the control law by solving for coil current vector $\mathbf{I}$ given transformation matrix $\mathbf{A}$ and control vector $\mathbf{F}$ in

$$\mathbf{F} = \mathbf{AI}. \tag{12}$$

The transformation matrix $\mathbf{A}$ is recalculated and matrix equation (12) is solved at each control update. If the computational speed of the control PC is not sufficient to solve the 6x6 matrix equation at 1000 Hz, a possible alternative approach is to precalculate inverse matrices at sampled motion intervals throughout the motion range of the levitated body in all translation and rotation directions as in [12], forming for example an approximately 300 MB lookup table if 10 sample points are selected across each of the 6 DOF.

VI. RESULTS

The proportional-derivative control gains used in position and orientation feedback magnetic levitation control are given in Table II. The device is pictured in Fig. 6 during levitation. Constant velocity motion trajectory results in all directions are shown using the position and orientation dependent current to force and torque vector transformations and gravity feedforward compensation as described in Section IV, in Fig. 7. The command velocities were 150 mm/sec and the command angular velocities 100 degrees/sec in all directions.

Small overshoots can be observed at the end of some of the constant velocity motions. A well-tuned state-space angular velocity estimator for each rotational DOF is expected to permit larger damping gains. Translational motions produce small disturbances in rotational DOF (and vice versa) because the center of mass of the levitated body is not located at the center of the coil sphere, where the control forces and torques are applied in the actuation model. Large oscillations can be seen in the roll angle when this angle approaches 15 degrees due to the saturation of one of the coil amplifiers. The feedforward gravity compensation torque at this angle results in the required current in one of the coils to surpass 4.0 Amperes, and when this limit is reached there is no additional current available for this coil to apply sufficient damping control. Fabrication of aluminum coils will greatly reduce the required torque to support the levitated body at high roll and pitch rotation angles, so that the full ± 30 degree rotation range in all directions of the design is expected to be attainable without saturating and overheating any of the coils.

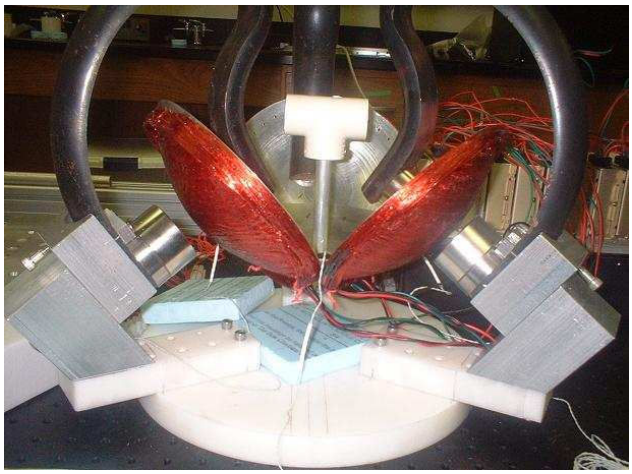

Fig. 6. Levitated Shell

VII. CONCLUSIONS AND FUTURE WORK

The motion control results from the ongoing development of this Lorentz levitation device and its control and interaction methods continue to be encouraging with regard to using the device for haptic interaction. The motion range of this device doubles the translation range and triples the rotation range of previous devices in all directions, providing ranges more similar to the motion ranges of an ball grasped and manipulated by the wrist and fingers.

Fabrication of a second levitated shell is currently in progress using aluminum rather than copper wire, to reduce the mass of the levitated bowl to 500 g or less, thereby improving its maximum acceleration capabilities and control bandwidths, and reducing the coil currents by approximately 50% and generated heat by 75%. More sophisticated control methods will be investigated such as modern state-space velocity estimation to improve damping control, and incorporating a spatial rigid body dynamics model for control of trajectories with much higher translational and rotational accelerations. Further improvement in motion and force control performance may also be possible by more accurate modeling of the spatial variations in magnetic flux between the magnets, which result in variations in the generated force magnitudes depending on the position of the levitated bowl. The levitation system has been integrated with the H3DAPI haptic programming interface, and current work is in progress to incorporate ODE real-time dynamic simulation to enable high-fidelity haptic interaction with real-time physical simulations of haptic skill tasks such as medical procedures.

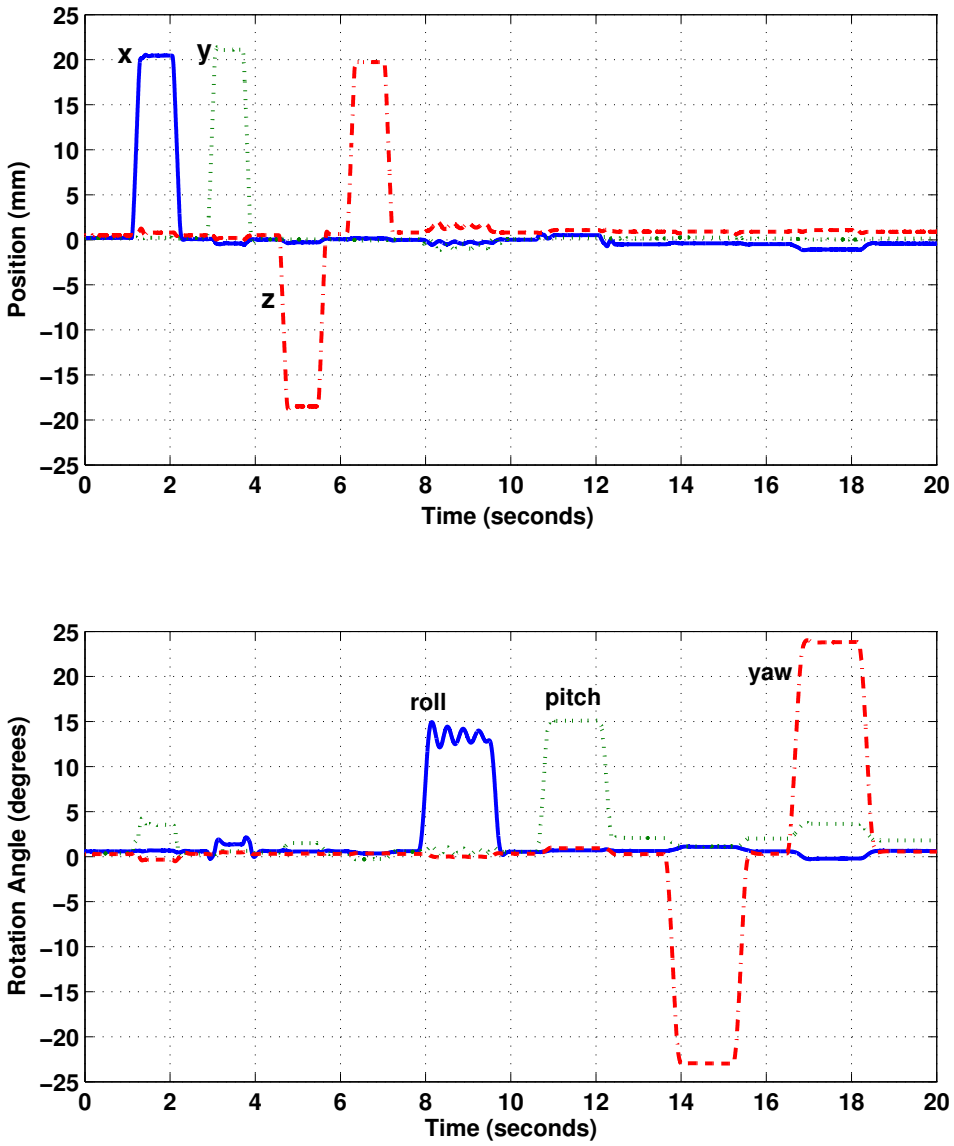

Fig. 7. Constant Velocity Translation and Rotation Trajectory Responses in All Directions

REFERENCES

[1] R. L. Hollis and S. E. Salcudean, "Lorentz levitation technology: a new approach to fine motion robotics, teleoperation, haptic interfaces, and vibration isolation," in *Proc. 6th Int'l Symposium on Robotics Research*, Hidden Valley, PA, October 2-5 1993.

[2] R. L. Hollis, S. Salcudean, and A. P. Allan, "A six degree-of-freedom magnetically levitated variable compliance fine motion wrist: design, modeling, and control," *IEEE Transactions on Robotics and Automation*, vol. 7, no. 3, pp. 320–332, June 1991.

[3] S. Salcudean and T. Vlaar, "On the emulation of stiff walls and static friction with a magnetically levitated input-output device," in *ASME IMECE*, Chicago, November 1994, pp. 303–309.

[4] S. Salcudean and N. Parker, "6-dof desk-top voice-coil joystick," in *International Mechanical Engineering Congress and Exposition*, Dallas, November 1997.

[5] P. J. Berkelman and R. L. Hollis, "Lorentz magnetic levitation for haptic interaction: Device design, function, and integration with simulated environments," *International Journal of Robotics Research*, vol. 9, no. 7, pp. 644–667, 2000.

[6] H. Zhang and C.-H. Menq, "Six-axis magnetic levitation and motion control," *IEEE Transactions on Robotics*, vol. 23, no. 2, pp. 196–205, April 2007.

[7] P. Berkelman, "A novel coil configuration to extend the motion range of lorentz force magnetic levitation devices for haptic interaction," in *IEEE/RSJ International Conference on Intelligent Robots and Systems*, San Diego, October 2007.

[8] P. Berkelman and M. Dzadovsky, "Extending the motion ranges of magnetic levitation for haptic interaction," in *Eurohaptics Conference and Symposium on Haptic Interfaces for Virtual Environment and Teleoperator Systems*, Salt Lake City, March 2009, pp. 517–522.

[9] V. Varadharajan, R. Klatzky, B. Unger, R. Swendsen, and R. Hollis, "Haptic rendering and psychophysical evaluation of a virtual three-dimensional helical spring," in *Symposium on Haptic Interfaces for Virtual Environments and Teleoperator Systems*, Reno, March 2008, pp. 57–64.

[10] E. Fasse, "On the spatial compliance of parallel manipulators and levitated platforms," in *ASME IMECE*, San Diego, April 1997.

[11] D. M. Y. Sommerville, *Analytic Geometry of Three Dimensions*. Cambridge: University Press, 1934.

[12] P. Berkelman and M. Dzadovsky, "Magnet levitation and trajectory following motion control using a planar array of cylindrical coils," in *ASME Dynamic Systems and Control Conference*, Ann Arbor, October 2008.